ARTICLE NO. 79-7038R

A80-058

40007
40010
60001

Hybrid Rocket/Airbreathing Propulsion for Ballistic Space Transportation

P.A. Kramer* and R.D. Bühler†
Institut für Raumfahrtantriebe, Universität Stuttgart, F.R.G.

The potential payload gains due to airbreathing propulsion are evaluated for a one-and-one-half stage reusable vertical-takeoff ballistic space transporter with a gross mass of 155 Mg. The system consists of a returnable ring of turborocket/ramjet engines added as a half-stage to the structure of a 130 Mg, single-stage, vertical-takeoff-vertical-landing, pure-rocket transporter considered in an earlier industry study. High-pressure topping-cycle rockets are used part-time in parallel with the airbreathers, with hydrogen/oxygen propellants used for both. With fixed takeoff mass and airbreathing engines, the main variables were the rocket thrusts and burning times, cycle change and staging points, and the injection angle at 100-m altitude. State-of-the-art technology was assumed. Trajectories free from constraints, except acceleration limits, allowed optimal propulsion system use. Propulsion performance maps, ascent trajectories, and weight breakdowns are given. Payload fractions up to 7.8% of gross mass were obtained for the airbreathing vehicle, which is very high for this size class compared with expendable two-stage rocket transporters.

Nomenclature

F	= thrust, force, N
g	= gravitational constant, m/s^2
I_s	= mass-specific impulse = $F/\dot{m}_p$, Ns/kg‡
Ma	= flight Mach number
$\dot{m}$	= mass flow rate, kg/s
n	= rotation rate, s^{-1}
p	= pressure, N/m^2 or Pa
p_{dyn}	= dynamic pressure = $\rho v^2/2$, Pa
T	= temperature, K
V	= flight velocity, m/s or km/s
γ	= trajectory injection angle
θ	= temperature ratio for reduced rpm = $T_t/T_{t,0}$
ρ	= density of the air, kg/m^3

Subscripts

∞	= freestream condition
C	= combustor
F	= fan
i	= injection
P	= propellant (fuel plus oxydizer)
S	= skin, surface
t	= total
0	= standard sea level conditions
1	= component entrance
2	= component exit

Acronyms

R	= rocket
RJ	= ramjet
TR	= turbo-rocket
GLOW	= gross liftoff weight (or mass)
LEO	= low Earth orbit (200 km)
SSTO	= single-stage-to-orbit
2-STO	= two-stage-to-orbit
VTOVL	= vertical-takeoff-vertical-landing
VTOHL	= vertical-takeoff-horizontal-landing
HTOHL	= horizontal-takeoff-horizontal-landing

Presented as Paper 79-7038 at the AIAA 4th International Symposium on Air Breathing Engines, Orlando, Fla., April 1-6, 1979; submitted June 27, 1979; revision received Dec. 27, 1979.

Index categories: Launch Vehicle Systems; LV/M Propulsion and Propellant Systems; Airbreathing Propulsion.

*Dipl.-Ing., Group Leader Combination Propulsion Systems. Member AIAA.

†Ord. Prof., Ph.D., Institute Director. Associate Fellow AIAA.

‡For the rocket, I_s equals the effective exit velocity in m/s. To obtain the weight-specific impulse in seconds, divide I_s by 9.81 m/s^2.

Introduction

THE purpose of this paper is a first evaluation of the possible improvements in payload of a certain class of space launchers through the use of rocket/airbreathing combination propulsion systems, specifically integrated turbo-rocket/ramjet engines. This is one, central part of a broader study reported earlier of the performance potential of such combination (or hybrid) propulsion systems (turbo-rocket, ramrocket) in comparison with pure airbreathing systems augmented (where necessary) with separate rockets.[1] Clearly, such comparisons can only be made on the basis of a definite mission and vehicle class. The reusable Earth-to-low-orbit space launcher has been chosen as one important sample mission for this comparison.

The possibility of utilizing airbreathing propulsion components for the atmospheric ascent portion of a space launcher has been considered since almost the inception of spaceflight. This was and is motivated by the fact that airbreathing engines offer about 8-20 times higher effective specific impulse values than pure rockets. Present-day (two-stage) rocket launch systems consume about 80% of their total propellant mass in the initial lifting and acceleration through the atmosphere to about 60 km and 2.3 km/s, which corresponds to an equivalent velocity increment of about 4.6 km/s or half of that required for reaching the low Earth orbit (LEO). A major portion of this large propellant mass could be saved with a partial use of airbreathing propulsion for the first stage. Though engine and structure weights would be increased, very substantial increases in payload (and payload fraction, the fraction of the gross mass that is payload) could be achieved with proper use of airbreathing engines, particularly for one-and-one-half or two-stage vehicles (see, for instance, Fig. 3-2. in Ref. 2).

The precise evaluation of potential gains in payload fraction with airbreathing engines requires simultaneous iterative variations of the propulsion system composition, the use cycles of the propulsion components, and the ascent trajectory, involving very extensive calculations to come near the attainable optimum. This was done here for one

promising propulsion system option and one size class and type of vehicle. The evaluation of the possible cost savings per kg of payload, while the ultimate goal, is far beyond the scope of the present study. However, the weight breakdowns and trajectories calculated here are necessary ingredients for future life-cycle cost determinations.

System Definition and Assumptions

Three possible types of reusable booster vehicles may be considered for airbreathing engines: VTOVL (ballistic), VTOHL, and HTOHL (winged vehicles). The VTOVL type and a relatively small "European size" vehicle (with a gross mass of 155 Mg) was chosen. The BETA IA project data[3] existed as a pure rocket comparison vehicle of this type and size class, and the adaption of the structure for the added integrated airbreathing engines appeared manageable. Also, the conical shape of the VTOVL vehicle lends itself best to the large aircapture and inlet areas required (Fig. 1). Relatively few published results exist on VTOVL boosters with airbreathing propulsion.[4-6] The majority of proposed airbreathing boosters are winged vehicles. For the HTOHL types (as, e.g., in the recent project studies of Refs. 7-10), the airload and structure calculations become a major part of the project, while the propulsion aspects were the primary interest here.

The turbo-rocket was chosen very early in this study. Through its high thrust density at low speeds,[1] this engine type appeared as the best supplement to the ramjet for the requirements of the ballistic ascent. The turbo-rocket consists of a fanjet engine, the turbine of which is driven by a fuel-rich high-pressure LH/LOX gas generator. The excess fuel is burned in an afterburner which becomes the ramjet combustor at higher Mach numbers. The engines and inlets are integrated into the vehicle structure so that the cone becomes part of the airinlet (Fig. 1).

A one-and-one-half stage vehicle was treated in detail in which the airbreathing engine portion is to be dropped at the end of its use, while the same rocket motors remain for the rest of the ascent and the landing. Recovery schemes for the dropped portion are believed possible but have not yet been designed. The effect of the recovery system mass on the payload can be estimated from Fig. 10, as discussed later.

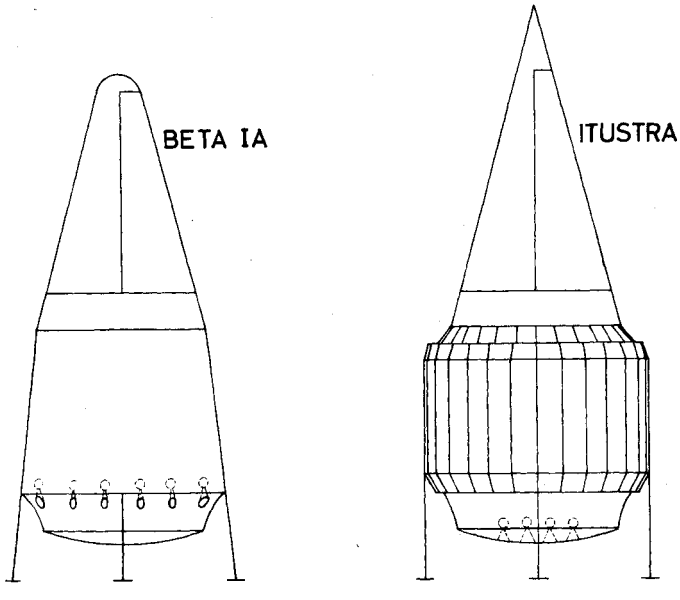

Fig. 1 (Left) BETA IA project: SSTO, VTOVL, baseline LH/LOX rocket vehicle, GLOW = 130 Mg,[3] length = 20 m, max diam = 9 m. (Right) ITUSTRA project (Integrale Turbo-Staustrahl-Rakete): 1½-STO, VTOVL, LH/LOX hybrid rocket airbreathing vehicle, GLOW = 155 Mg, length = 23 m, max diam = 9.8 m.

The single-stage-to-orbit version was too marginal for the size class and other assumptions chosen here, though this might be attractive for much larger sizes and more advanced technology concepts.[4,6-8,10]

All important technical limits and performance parameters in this study, e.g., temperatures, pressure, heat loads, structure weights, etc., were chosen at or near current state-of-the-art values. This also pertains to the propulsion components—compressor, turbine, combustion chamber, and inlet—even though such turbo-rocket systems as a whole may not exist as yet to our knowledge. While this preliminary design basis appears as rather conservative for the time frame in which such systems would be built, it should allow for uncertainties inherent in a new system, and thus increase the confidence level in the conclusions.

The approach chosen for this study was to start with a well worked out pure rocket VTOVL space transport as the baseline vehicle, and to calculate the necessary modifications for the addition of airbreathing propulsion and the resulting changes in the payload delivered to LEO.

Twenty-eight airbreathing engine modules have been grouped around the modified lower portion of the BETA IA vehicle. The conical upper portion of the vehicle together with ramps form the inlet. Each airbreathing engine module consists of its inlet, a hydrogen/oxygen turbo-rocket with afterburner, an adjustable nozzle, and a bypass duct with flaps to close off the turbo-rocket and allow the engine to operate as a pure ramjet. The adjustable primary nozzles lead to a common plug-type secondary nozzle.

The rocket engines are high-pressure LH/LOX topping-cycle engines, similar to those of the baseline vehicle or the space shuttle main engine (SSME), with two-position nozzles integrated into the base of the plug, which serves as a heat shield for re-entry. The number of these rocket engines used was varied during the study.

The following other basic assumptions and sources of data were used:

The variable ramp (two-dimensional) inlets were calculated as in Ref. 7, using the flow conditions behind the conical shock as the inlet conditions. The maximum lip entrance area is limited to the maximum cross section of the vehicle.

The variable thrust nozzles were assumed to expand to ambient pressure where possible or to the vehicle's maximum cross section at higher Mach numbers.

For the three-stage transonic fan, the performance map of an existing fan of 70-cm diameter was used.[11] The fan exit temperature was limited to 1000 K. When this was reached, either the reduced rotational speed ($n/\sqrt{\Theta}$) was decreased or the cycle change to ramjet executed. In the cases presented here, the best cycle change points (to ramjet) generally occurred prior to reaching this limit.

The turbo-rocket gas generator was assumed to operate at 100 bar, fuel-rich to produce 1100 K and sufficient mass flow as required by the fan power. The turbine is conventional with the preceding inlet conditions.

The internal flow, combustion, and internal ("gross") thrust calculations were discussed in detail in Ref. 1. Very briefly, real gas properties were used throughout with dissociation included where applicable, combustion according to Ref. 12, and partially frozen flow in the nozzle expansion with defined freezing point cross checked with the Bray criterion.[13]

The aerodynamic drag for the cone-shaped vehicle has been calculated from semiempirical functions based on data from several sources.[14] The base pressure on the vehicle was accounted for in the thrust calculation.

Tangential thrust only and no aerodynamic lift or angle of attack was used during the airbreathing part of the trajectory. For the pure rocket upper trajectory thrust magnitudes and angles, according to the simplified optimization method, the so-called "tangent beta law"[15] was used. Lift forces and drag variations due to angle of attack were neglected for these upper trajectory integrations.

The masses of the airbreathing engine assemblies were estimated from internal statistical data collections on similar components, and the resulting mass-to-thrust ratios agree with comparable turbo-rockets discussed in the literature. The mass of the basic vehicle structure was taken from the BETA IA study[3] with no deductions for deleted fuel tanks since the unused fuel volume was considered necessary for the increased payload. Mass variations due to the variable number of rocket engines used were accounted for as a final correction to the payload.

The approach used in this study is characterized by two important premises:

First, the number and size of the airbreathing engines and the takeoff gross mass of the vehicle (155 Mg) were held constant, resulting in a fixed ratio of airbreathing takeoff thrust to gross weight of 1.34, similar to that of the comparison (baseline) rocket vehicle. Varying numbers of additional rockets were added to approach an optimum. Fuel plus oxidizer masses required were then calculated for each ascent (plus reserves for control and landing) and the remaining mass to make up 155 Mg regarded as possible payload.

Second, the ballistic ascent trajectories were a priori left perfectly free to be derived from the chosen propulsion system combination and mode of use. In this point of approach, this study differs from most others in which the ascent trajectory is predetermined by flying, for example, along a line of constant dynamic pressure or within a narrow corridor in the altitude flight-speed plane. Only the largest allowable acceleration (4.5 g) was prescribed, compared with 3.8 g for the baseline vehicle. This approach which allows each system variation to find its own ascent trajectory, while much more demanding in computing time, appeared to be superior in permitting the optimal use of the propulsion system within assumed constraints. A predetermined (e.g., constant dynamic pressure) trajectory implies in the authors' opinion unnecessary throttling, and thus nonoptimal utilization of the heavy airbreathing engines even prior to reaching the acceleration limit. The price for a free trajectory is that complete performance maps of the airbreathing systems (with all possible cycle variations) and of the rockets have to be precalculated in sufficient detail (or point density) for the whole velocity and altitude spectrum to allow any ascent trajectory to be "flown" through by integration.

The only predetermined trajectory component, typical for rockets, was a 100-m vertical climb followed by a variable injection angle maneuver. It is clear that the inclusion of angles of attack and the resulting substantial lift forces will

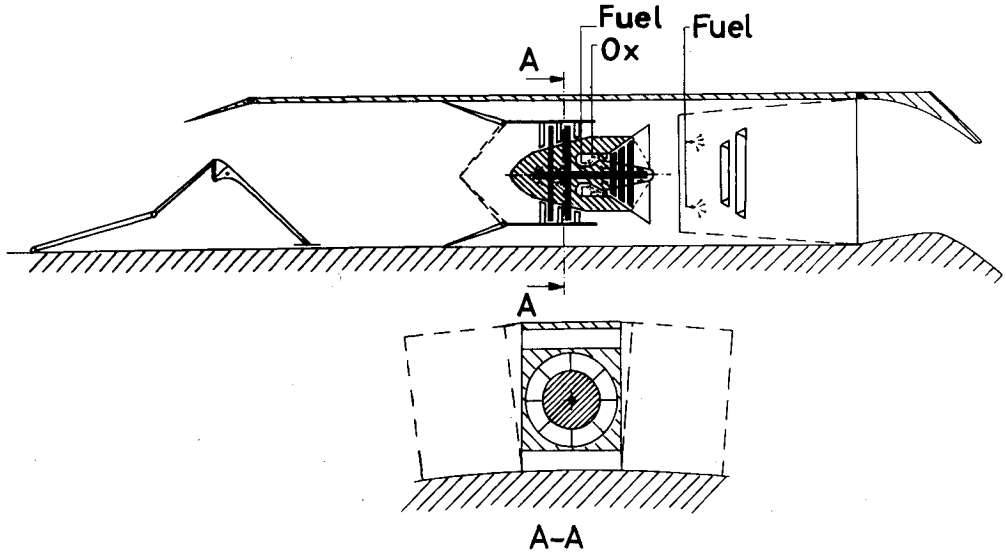

Fig. 2 Integrated turbo-rocket/ramjet engine module configuration.

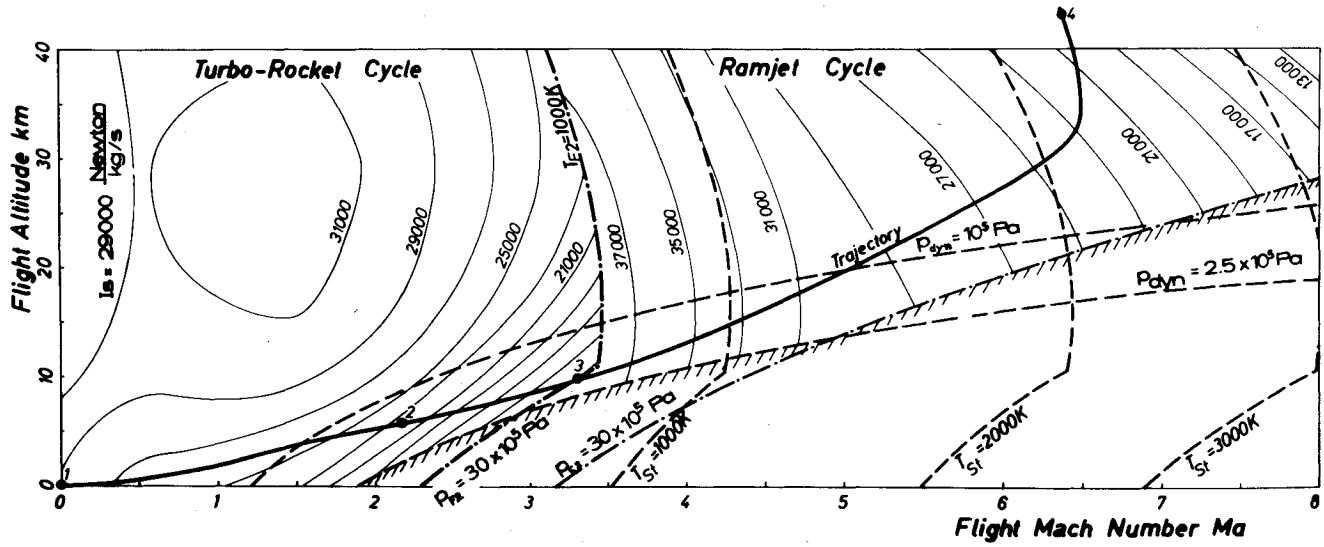

Fig. 3 Typical turbo-rocket/ramjet engine performance map with a typical trajectory and limiting lines for the engine and the structure: 1, liftoff; 2, boosting rocket engines off; 3, end of turbo-rocket operation, cycle switching; 4, staging (airbreathing engine mass only).

later permit a wider choice of trajectories than the purely ballistic ones to limit structural heat loads. Here, this additional variable would have greatly complicated the calculations and introduced additional uncertainties in drag and engine performance, and did not appear essential for the primary purpose of the study.

The original assumption of the fixed number, size, and thrust of the airbreathing engines was based partly on structural and capture area considerations and partly on the initial attempt to fly with airbreathers alone if possible. While this proved not feasible with the installed engines and gross mass, the assumption still appears quite good now for two reasons. First, the additional rockets required for optimal payload turned out to be close to those required in any case for the upper trajectory. Second, over portions of the upper trajectory the thrust of the turbo-rockets and even that of the pure ramjets becomes excessive for 4.5-g acceleration and must be throttled (as shown later) so that additional air breathers would very likely have represented wasted dead weight. However, this airbreather fraction should later be optimized.

The percentage of the total liftoff thrust provided by the rockets and the injection angle (at 100 m) were taken as the free variables. Other variables were the rocket thrust during the airbreathing ascent, the switchover points from turbo-rocket to pure ramjet operation, assumed here to take place simultaneously for all engines, and the rotational speed $(n/\sqrt{\Theta})$ of the turbo-rocket engine. Throttling or cutting out some portions of the airbreathing engines also had to be introduced to avoid excess accelerations.

It is clear that with this large number of variables an almost limitless number of possible trajectories could be calculated. The following approach is an attempt to come, with an acceptable investment of computing time, sufficiently close to the best performance to evaluate the potential merits of the system.

Initial Results—Reference Point System

Integrated performance maps of the turbo-rocket and the ramjet configurations of Fig. 2 are shown in Fig. 3, separated for clarity here along the line of limiting fan outlet temperature (1000 K). The limit lines for 30×10^5 Pa afterburner pressure with and without fan as well as certain dynamic pressure (1.0 and 2.5×10^5 Pa) and stagnation temperature lines (indicating vehicle skin loading) are also shown, all using the computer evaluation method of Ref. 16.

One typial integrated ascent trajectory is shown, based on a 60% rocket thrust at liftoff and an injection angle of 68 deg. In this case, the cycle switching to ramjet (point 3) occurred at the 30×10^5 Pa combustor limit line. Already at point 2 (Mach 2.2) the rockets were cut off. It is important to note that at the higher speeds this typical trajectory rises quickly above 10^5 Pa dynamic pressure line, so that the crossing of the afterburner pressure limit in the ramjet regime ($P_{C2}=30\times10^5$ Pa) is avoided. Thus, these trajectories generally do not lead to the requirement for a scramjet system. In the example shown, stage separation is optimal at point 4, at Mach 6.3, and 43.5 km. Some lower (flatter) trajectories did get into the scramjet regime, but yielded smaller payloads to LEO (200 km) without scramjet engines. These results hold only for ballistic vehicles, whereas for winged vehicles using aerodynamic lift during ascent, the opposite has been shown in various studies and the use of the scramjet regime would become advantageous.[4,6-8]

In Fig. 4, a few selected cases of the large number of trajectories investigated are shown. Since no interesting solutions with the turbo-rockets alone were found within the assumptions, additional rocket thrust, here between 41 and 67% of the total liftoff thrust, was applied for the start. High-pressure topping-cycle rockets are preferred for this purpose here, as in another recent paper,[8] instead of the ejector ramjet or ducted rocket approaches tried earlier.[6,7] This is because the high-pressure simple rockets perform and fit much better for the subsequent ascent outside of the atmosphere where they have their main use.

Figure 4 shows that for each percentage of rocket thrust at liftoff there is a limited range of possible injection angles and one (or sometimes two) optimum angle(s). These points of highest payload form a rather flat envelope which peaks at about a 68-deg injection angle and a 60% rocket thrust at launch. This point has been chosen as an initial reference point.

Figures 5 and 6 show details of the thrust, specific impulse, and various cycle switching points. Figure 5 shows the rapid increase of the turbo-rocket thrust with increasing flight speed. At about Mach 2.0, where the turbo-rockets have quadrupled their thrust, the rockets are turned off in steps. Shortly thereafter the thrust of the turbo-rocket approaches 10×10^6 N (or 5 times sea level static value) and the assumed acceleration limit of 4.5 g is reached. The turbo-rockets are then cut off in steps until the cycle switching point to the ramjets at 10.4-km alt and Mach 3.4. Here, this cycle change to ramjet is carried through for all engines simultaneously, but in future runs this could be done in steps and started earlier. The ramjet thrust is lower at first but rises again to the acceleration limit, so that now part of the ramjets has to be turned off (or throttled). Between 18- and 28-km alt, the ramjets are gradually all turned back on (or turned up to maximum thrust). From there on, the ramjet thrust drops to nearly negligible value at 43 km where staging takes place (i.e., the airbreathers are dropped) and the rockets (about 80% of those installed for liftoff) take over. A speed of only 2.044 km/s was reached with the airbreathing propulsion in this case.

In Fig. 6, the same reference point ascent trajectory can be followed in the specific impulse diagram. The combined effective specific impulse rises from about 3/2 of the rockets' value at liftoff to that of the turbo-rocket. It then drops rather steeply to about 11,800 Ns/kg at the cycle switching point. This was a bad operation mode and regime for the turbo-rockets; they operated very fuel-rich in this regime and should have been replaced by the ramjets much sooner. The ramjets then bring good specific impulse until the staging point. These diagrams indicate the further improvements which can be made over the reference point run, as will be shown in the following paragraph.

Payload Sensitivity to Various Influences

Optimum Staging and Cycle Switching

In Fig. 7, all local maxima of the curves of Fig. 4 (connected with the envelope curve) have been optimized with

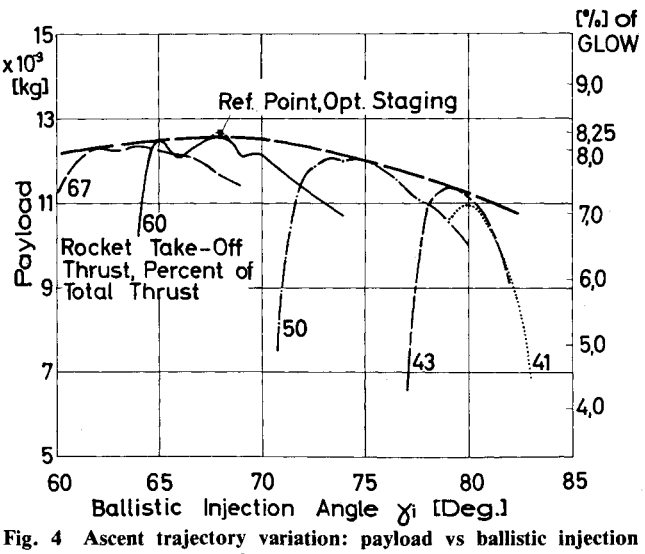

Fig. 4 Ascent trajectory variation: payload vs ballistic injection angle for several boost rocket thrust percentages.

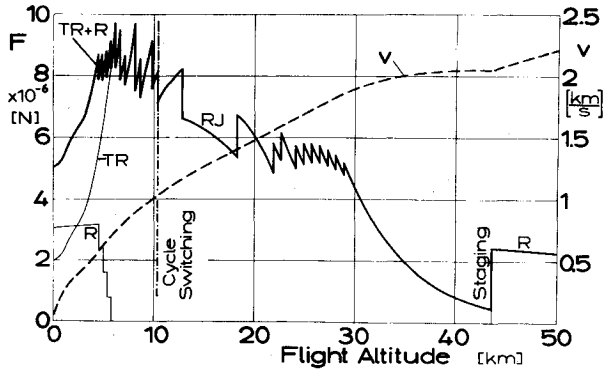

Fig. 5 Thrust and velocity profile over the flight altitude for a typical ascent trajectory (ref. point case, Figs. 3 and 4).

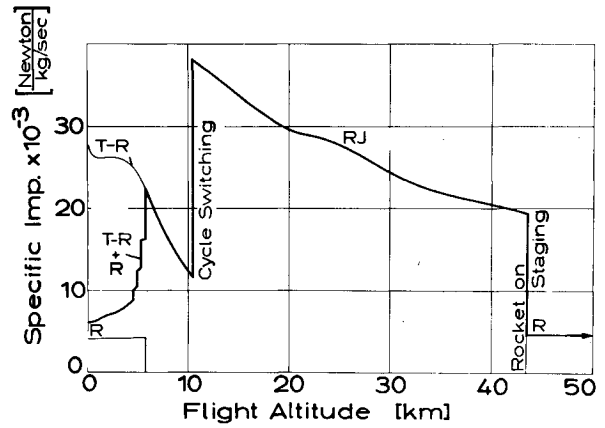

Fig. 6 Specific impulse profile over the flight altitude for a typical ascent trajectory (ref. point case, Figs. 3 and 4).

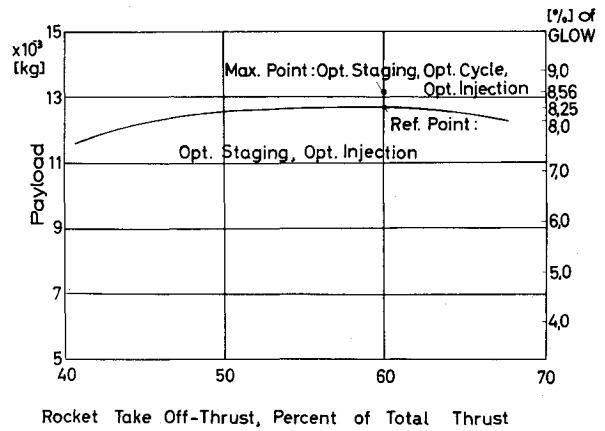

Fig. 7 Payload vs boost rocket thrust percentage. Envelope curve for optimum staging and optimum injection angle. Max point shows influence of optimum engine cycle switching.

respect to stage separation, as it had been done for the reference point only in Fig. 4. The new envelope curve in Fig. 7 contains this reference point with its 8.25% payload fraction. This revised envelope is still flatter than that of Fig. 4, so that a choice of the 50% rocket case, as will be discussed, becomes even more attractive.

However, the reference point case has been chosen as a basis of comparison for all the following variables because of its absolutely best payload value up to that point.

First, variations of the cycle switching point from turbo-rocket to ramjet were investigated, still for all engines at once. Up to this point, the cycle change was done automatically by the computer when either the fan outlet temperature or the

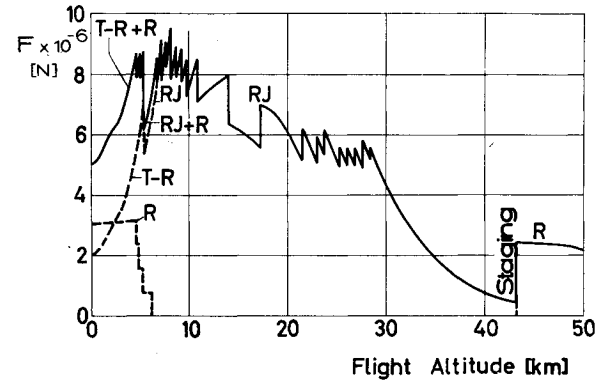

Fig. 8 Thrust and velocity profile over the flight altitude for the max point case (Fig. 7).

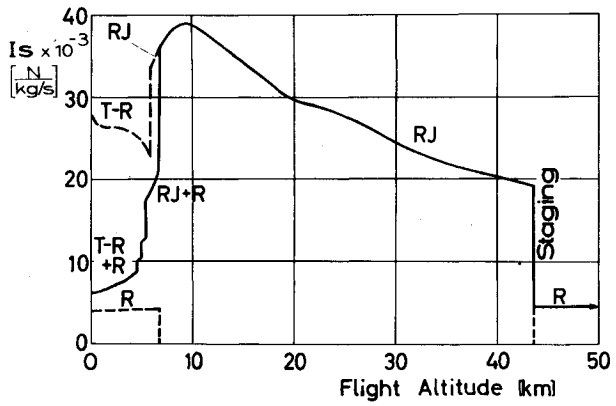

Fig. 9 Specific impulse profile over the flight altitude for the max point case (Fig. 7).

combustor pressure limit was reached, but it became clear from Figs. 5 and 6 that earlier switching would improve the overall specific impulse. The cycle switching was first located according to the best combined specific impulse (rockets plus airbreather) and then according to the best payload of the integrated trajectory. Both approaches lead to a much earlier changeover from turbo-rocket to ramjet, so that the drop in specific impulse shown in Fig. 6 (due to fuel-rich operation of the turbo-rocket) is avoided.

Figures 8 and 9 show the thrust and specific impulse variations along the ascent trajectory with optimized cycle switching point. So far in the program, the parallel booster rockets were cut off in 25% steps when the acceleration limit was reached. Retaining this procedure, the optimum cycle change point lies just ahead of the rocket cutoff. The final gain in payload for the trajectory based on the runs of Figs. 8 and 9 was 4.6%, that is, from 8.25-8.56% payload fraction. This value shown as the highest point in Fig. 7, however, has to be corrected for certain weight additions, as will be discussed.

Some further possible improvements become evident from Figs. 8 and 9. First, at one point, the same thrust at higher specific impulse could have been obtained with the turbo-rockets rather than with rockets and ramjets combined. Thus, the rocket cutoff must be introduced as a variable rather than being based on acceleration limit. Second, the last ramjet cutback at about 13-km altitude could have been avoided since the ramjets reached their peak thrust at about that point. Third, throttling of the ramjets by reducing fuel/air ratio rather than cutting off complete engines would improve the overall specific impulse. Finally, the stage separation could be delayed and the ramjets used to higher speeds and altitudes if part of the rockets were operated in parallel again before stage separation. These refinements could not be included in time for this paper.

Some attempts to improve the specific impulse by reducing the rotational speed of the turbo-rocket were not successful presumably because these speed reductions were applied at points too early along the trajectory where the rockets were still in use. With the advanced cycle change to ramjet operation, the turbo-rocket speed has lost some importance as a variable for optimization.

Numerous other variations, including those just mentioned, can of course be tried, and some of these calculations will be carried out in the future after a thorough further analysis of the results obtained to date. Since a general theory for optimizing a transport system of this type is far from a practical reality, one must rely on a purely numerical ("cut-and-try") approach used here, which involves a rather large number of complete integrations with each new variable introduced.

It should be mentioned here that the upper pure rocket portions of the trajectories (after staging) were so far calculated with an acceptable but relatively simple optimization procedure, as earlier pointed out. For the future, the analysis model for the upper trajectory must be refined simultaneously with finer optimization of the airbreathing portion.

Sensitivity to Engine Mass Variation and Mass Correction

The results presented so far have to be corrected for the varying rocket motor mass in those cases where more than 50% of the total liftoff thrust was assumed to come from the parallel rockets. Rockets amounting to 50% of liftoff total thrust are considered necessary for the upper trajectory, and thus included as a constant even where not fully used at launch. The mass of any additional rockets (e.g., 10% of liftoff for the reference point case) has to be deducted from the payload. The additional rockets are assumed to be staged-off with the airbreathing engines, reducing the payload fraction of the reference point from 8.25-7.87% of GLOW.

In order to investigate the payload sensitivity to the statistically based mass of the airbreathers, this mass has been varied also at the reference point case. The result is a linear connection between payload and airbreather mass (Fig. 10). A 25% increase in propulsion system mass would result in a payload loss of 12%, for example.

This discussion gives additional information on how the payload might be reduced due to the masses of a recovery system—parachute, fins, fuel, etc.—for the staged-off airbreather engine cluster. This important problem has not yet been investigated, as previously stated. The recovery of the rest of the vehicle is included already in the structure analysis of the baseline vehicle.[3]

Aerodynamic Drag

The payload sensitivity to the aerodynamic drag assumption has been investigated over a wide range. The results, referred to the reference point case, are shown in Fig. 11. The payload gain in the case of the reduced drag is relatively small, for example, 7% more payload with 50% drag reduction. On the other hand, the payload would decrease rapidly in the case of the drag increasing by more than 50%. Drag increase could be offset partly by increasing thrust.

Table 1 Mass breakdown of final system in kg

Dry mass of the baseline vehicle[3] (structure, re-entry heat shield, electronics, secondary propulsion, etc.)	(10,000)	
Net mass of the baseline vehicle[3] (dry mass plus propellant reserves and recovery propellant for the core vehicle)		12,400
Additional rocket mass for atmospheric ascent	(1402)	
Airbreather engine mass	(24,851)	
Stage separation mass (½-stage)		26,253
Propellant mass for atmospheric ascent	(31,601)	
Propellant mass for ascent in space	(72,569)	
Total propellant mass for ascent into LEO (nominal mass)		104,170
Payload in orbit (LEO) (only core vehicle recovery, no payload)		12,128
Gross liftoff weight (GLOW)		154,951
Payload fraction (payload to GLOW) ITUSTRA (1½-STO)		7.83%

Finally Selected System and Comparison with Pure Rocket Transporters

The maximum point of Fig. 7 has been corrected for the added rocket masses, as discussed for the reference point. This correction has involved a number of trajectory iterations. Table 1 gives a mass breakdown of the finally selected vehicle and trajectory.

For comparison, the pure-rocket SSTO VTOVL baseline vehicle BETA IA[3] has the characteristic values shown in Table 2 with about 2.1% payload.

The predecessor project of BETA IA with an even smaller size was the SSTO VTOVL project SASSTO.[17] With a more advanced lightweight structure and again LH/LOX as propellants, this project predicted a much higher payload fraction of 3.6%.

Another project study vehicle of comparable size was the expendable, two-stage Europa III-D[18] with high-pressure topping-cycle rocket and LH/LOX in both stages, with 5.75% payload. The Europa III-E2 was a competitive project study with similar technology but parallel staging, allowing a kit-type construction philosophy.[19]

Compared to the SSTO BETA IA baseline vehicle, the 1½-STO ITUSTRA-vehicle has a 3.76 times higher payload fraction; compared to the payload fraction of the expendable 2-STO vehicle project Europa III-D, the factor is 1.41. The

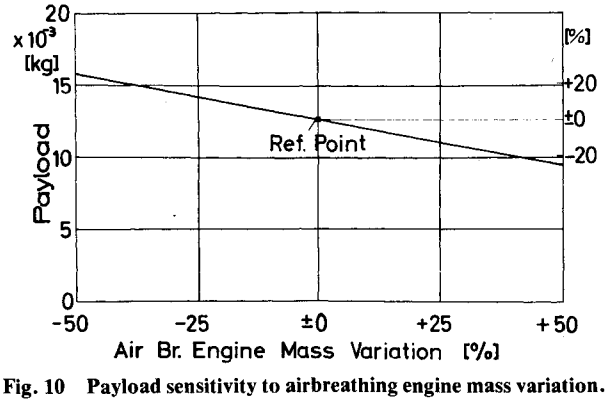

Fig. 10 Payload sensitivity to airbreathing engine mass variation.

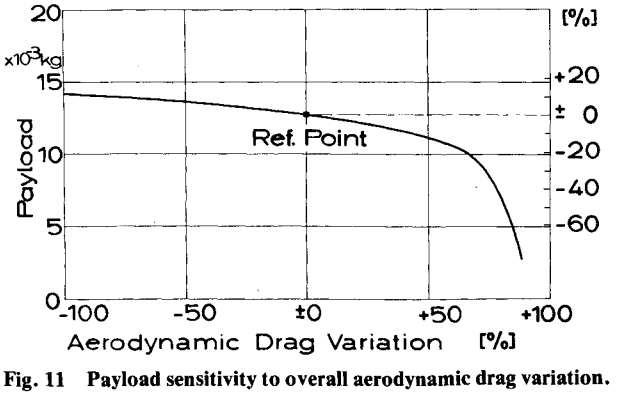

Fig. 11 Payload sensitivity to overall aerodynamic drag variation.

Table 2 Project ITUSTRA compared with other systems or projects

Project, company	Stages	Launch/ recovery	GLOW, kg	Payload in LEO, kg	Payload % of GLOW
ITUSTRA	1½	VTO/VL parachute	154,951	12,128	7.83
Pure rocket project vehicles of comparable size with LH/LOX as propellants					
BETA Ia, MBB[3]	SSTO	VTO/VL	130,100	2700	2.08
SASSTO, Douglas[17]	SSTO	VTO/VL	98,000	3500	3.57
Europa III-D, ASAT (MBB/ERNO)[18]	2 (tandem)	VTO/ expendable	87,000	5000	5.75
Europa III-E2 (ELGO IV), Dornier System[19]	3 (parallel)	VTO/ expendable	84,000	5000	5.95
Sample present-day space transporters of different size and technology					
Space Shuttle[a]	2½	VTO/HL parachute	1,992,500	29,500	1.48[a]
Titan IIIC	4	VTO/ expendable	640,000	11,400	1.78
Ariane	3	VTO/ expendable	200,933	4500	2.24

[a] Man-rated, payload recovery, high reusability, therefore nor directly comparable.

additional mass for a recovery system for the airbreathing engine cluster is not expected to change this picture too much.

For additional comparisons, a few present-day space transporters of completely different size and technology are also listed in Table 2. To this it should be remarked that for the Space Shuttle with its man-rated cabin, payload recovery capability, and high reusability, the term payload has a different meaning and the number is not directly comparable.

To evaluate the results presented here, it should be emphasized again that the rather high-payload fraction of the turbo-rocket/ramjet vehicle was obtained in spite of the small size and the assumption of the state-of-the-art technology for the propulsion components and the structure. Larger vehicles are known from past experience (e.g., the Saturn class) and from recent design projects to yield higher payload fractions due to higher structural efficiency.

Advanced technology, such as control configured ultralight structures, would substantially improve both pure rockets and airbreathers alike. However, advanced technology propulsion components, such as scramjet engines for the upper portion and lightweight turbo-rocket engines using single-stage supersonic compressor-diffusers for the lower trajectory, should give an added advantage to the airbreathing systems; engine weight and technology generally play a more dominant part here, and higher velocity gain in the atmosphere, (with scramjets) if without undue weight penalty, is clearly desirable. The range of payloads given in the literature for both airbreathing and pure rocket heavy-lift vehicles (for example, Refs. 2, 4, 7-10, 20, 21) substantiate these statements.

Conclusions

Airbreathing propulsion was found to be feasible for VTOVL space transporters.

A one-and-one-half or two-stage vehicle allows the real potential of airbreathing propulsion for the VTOVL transporter to be realized, whereas with SSTO systems much of the gain of the airbreathing propulsion phase is lost again due to excessive dead weight in the upper trajectory.

The turbo-rocket with its known high thrust density[1] and high thrust-to-weight ratio at low flight speeds, combined with good specific impulse, appears as a promising complementary engine to the ramjet for the ballistic ascent mission.

Parallel burning rockets during the launch phase have so far been found necessary or at least advantageous for this transporter concept.

Hydrogen fuel is favored for its high specific energy and its lean burning capability for throttled ramjet operation. The low-density penalty is insignificant here due to the small amount of propellant (about 20% of GLOW) used during atmospheric ascent.

The free ascent trajectory used here, in contrast to many other studies, appears to offer considerable advantage through more optimal use of the airbreathing propulsion system, thereby justifying the higher computing time investment.

The injection angle used was found to be rather critical for the ballistic ascent trajectory and depends on the amount of rocket thrust used during launch.

Scramjet propulsion did not appear necessary for the trajectories investigated.

The proposed modular airbreathing system would allow the use of existing-size engine components, and thus immediate full-scale engine development and testing with existing facilities. The two-dimensional inlets and nozzle portions may simplify achieving the needed cross-sectional control.

Very attractive payload capabilities even for small vehicle sizes and state-of-the-art technology levels were found to be possible with turbo-rocket/ramjet propulsion systems. A fully reusable shuttle transporter of modest ("European") size thus becomes an interesting possibility.

Definite further improvements appear possible within the present assumptions of size and technology level through further propulsion cycle and trajectory optimization, as pointed out in the text. The inclusion of angle of attack and lift forces, while complicating the optimization, may bring payload gains and will also permit structural load considerations to be better accommodated.

Availability of advanced technology, such as scramjet engines and a single-stage supersonic compressor-diffuser with high-speed turbine in addition to lighter heat-resistant structures, may in the future further increase the payload margin of the airbreathing systems relative to pure rockets through higher energy gain in the atmosphere and reduction of empty weights.

Acknowledgments

The authors wish to thank the Deutsche Forschungsgemeinschaft and the University of Stuttgart for the continuing support of this project as a part of the Sonderforschungsbereich 85. A travel grant by the U.S. Air Force and U.S. Navy is gratefully acknowledged.

References

[1] Kramer, P.A. and Bühler, R.D., "Integrated Turbo-Ramjet/Rocket Performance Potential—Project ITUSTRA,"

ICAS/DGLR Paper No. 76-045, 3rd Internal Symposium on Air Breathing Engines, Munich, West Germany, March 7-12, 1976.

[2] Bühler, R.D. and Lo, R.E., "Raumfahrtantriebe—heutige Leistungsgrenzen und Einsatzfähigkeit sowie Entwicklungstrends," Deutsche Gesellschaft für Luft-und Raumfahrt, DGLR Paper No. 78-108, 1978.

[3] Koelle, D.E., et al., "Durchführbarkeitsstudie über ein ballistisches, wiederverwendbares Trägersystem—BETA," Messerschmidt-Bölkow-Blohm GmbH, Bericht-Nr. UR-V-025(69), 1969.

[4] "A Forecast of Space Technology 1980-2000," NASA SP-387, Jan. 1976.

[5] Woodis, W.R., "Performance Considerations for a VTOVL Boost Vehicle Using Turbo-Ramjet Engines," *Ballistic Missile and Space Technology, Vol. IV: Re-entry and Vehicle Design,* Academic Press, New York and London, 1960, pp. 205-254.

[6] Escher, W.J.D., "Composite (Rocket/Airbreathing) Engines: Key to the Advanced (Non-Staged) Space Transport Vehicle," presented in "A Short Course in Reusable Launch and Reentry Vehicles for Space Flight," The University of Tennessee Space Institute, Tullahoma, Tenn., Aug. 1969.

[7] Bendot, J.G., Brown, P.N., and Piercy, T.G., "Composite Engines for Application to a Single-Stage-to-Orbit Vehicle," NASA CR 2613, Dec. 1975.

[8] Martin, J.A., "Ramjet Propulsion for Single-Stage-to-Orbit Vehicles," Society of Automotive Engineers, SAE Paper 77-1011, 1977.

[9] Jackson, L.R., et al., "A Fully Reusable Horizontal Takeoff Space Transport Concept with Two Small Turbojet Boosters," NASA TM-74 087. Oct. 1977.

[10] Hanley, G.J. and Bergeron, R., "An Overview of the Satellite Power System, Transportation System," AIAA/SAE Paper 78-975, AIAA/SAE 4th Joint Propulsion Conference, Las Vegas, Nev., July 25-27, 1978.

[11] Volkmann, H., Fottner, L., and Scholz, N., "Aerodynamische Entwicklung eines dreistufigen Transsonik-Frontgebläses," Deutsche Gesellschaft für Luft-und Raumfahrt, *Zeitschrift für Flugwissenschaften,* Vol. 22, April 1974, pp. 135-144,

[12] Gordon, S., and McBride, B.J., "Computer Program for Calculation of Complex Chemical Equilibrium Compositions, Rocket Performance, Incident and Reflected Shocks, and Japman-Joguet Detonations," NASA SP-273, 1971.

[13] Bray, K.N.C., "Atomic Recombination in a Hypersonic Wind-Tunnel Nozzle," *Journal of Fluid Mechanics,* Vol. 6, No. 1, 1959, pp. 1-32.

[14] Cellard, M., "Abschätzung eines Widerstandskoeffizienten als Funktion der Machzahl eines Kegels im Unterschall-überschallbereich," Institut für Raumfahrtantriebe, Universität Stuttgart, West Germany, Interner Bericht Nr. IRA 77-IB5, 1977.

[15] Bryson Jr., A.E. and Ho, Y.C., *Applied Optimal Control,* Blaisdell Publishing Co., Waltham, 1969, pp. 59-63.

[16] Hartwig, R., "Hyperbolic Data Representation and Analysis (HYDRA)," *Eurographics 79,* Bologna, Italy, Oct. 25-27, 1979; also "Fast Interactive Analysis of Three-Dimensional Arrays," personal communication, IBM Research Center, Heidelberg, F.R.G., 1980.

[17] Bono, P., "The Enigma of Booster Recovery—Ballistic or Winged?," SAE Space Technology Conference, Palo Alto, Calif., May 1967.

[18] "Vergleiche zu Europaträger-Vorschlägen, hier: Europa III-D," ASAT (MBB/ERNO), Appendix in Ref. 19.

[19] Reichert, R.G., Drtil, A., et al., "Europaträger III-E2 ELGO," Auftrag des Bundesministeriums für Bildung und Wissenschaft, Auftrag RFT 1020, Dornier System GmbH, Friedrichshafen, West Germany, Dec. 1969.

[20] "Solar Power Satellite System," Definition Study Pt. 1, Vol. 5, SPS, Transportation Representative System Description, Boeing Aerospace Co., Seattle, Wash., NASA CR-15-1558, July 28, 1977.

[21] Koelle, D.E., "Performance and Cost Analysis for an SSTO + OTV Cargo Transportation System to Geosynchronous Orbit," IAF Paper 78-A-27, 1978.